CRYOGENIC TEMPERATURE EFFECTS ON PERFORMANCE OF POLYMER COMPOSITES

David Hui* and P.K. Dutta**

October 2002

* Dept of Mechanical Engineering, University of New Orleans, New Orleans, LA 70148
** U S Army Engineer Research and Development Center, CRREL, Hanover NH 03755

1. INTRODUCTION

The objective of this study is to evaluate the low temperature behavior of polymer composites down to the cryogenic temperature range. This would be accomplished by study of its behavior in several ways. First we would study the microfracture growth by observing the acoustic emission as the temperature is lowered. We would also note any damage growth by ultrasonic velocity testing applying the pulse echo method. Effects of such low temperature would then be studied by examining the shear properties by the short beam shear test, and also the fracture toughness properties over a wide range of strain rate and temperature. At present these studies are continuing. The limited data obtained from these studies are reported in this report.

2. BACKGROUND

In near future the lightweight composites will be used in the NASA re-entry vehicles. The structural systems of such re-entry vehicles must withstand rapid loading, vibration, high acceleration at take off from launching platforms in most severe environments, while internally containing liquid oxygen and hydrogen at cryogenic temperatures. Polymer composites, a multiphase material will be subjected to extremely high differential stresses within the phase components itself. In the past, careful manufacturing condition under controlled pressure and temperature in the autoclave systems provided reasonably satisfactory control of development of micro cracks during curing and subsequent applications in severe temperatures. In the new low cost, high volume manufacturing process, called the VARTM (Vacuum Assisted Resin Transfer Molding) process, control of the development of residual stress induced micro fracture will be extremely difficult. Research is needed to characterize such microstructures, monitor development and progression of the micro cracks under cryogenic temperature and service conditions, and finally assess the influence of such fracture growths on the performance of such structures by fracture mechanics studies. The current research program address some of these issues.

2.1 Failure modes

The primary concern for composites being used in the new generation of the re-entry vehicles is not only premature failure, but that they must not leak excessively even after multiple launches. Composites in space applications, whether used as rocket shell, satellite structures, or sensor platforms involve extremely high temperature and load variation at extremely high rates not only on its surface, but also through the thickness. Thick-section composites typically fail at stresses and strains that are well below the expected failure limits. Delamination is a common mode of failure. When cold, they fail with very small amount of strain, with more violence and high-energy release. This early failure is often attributed to the existence of critically sized processing and/or material defects and interfacial problems in the interphase region between the matrix and the reinforcing phase (Drzal 1983, 1986; Sottos 1990; Palmese 1992; Skourlis

1995; Hrivnak 1996; Harik 1997; VanLandingham 1997; Fink and McCullough 1999). Evaluation of interphasial mechanical properties has been carried out experimentally (Sottos 1990; VanLandingham 1997) and theoretically (Palmese 1992; Chu and Rokhlin 1996). The extent of the interphase region in composites is significant (Hughes 1991). For instance, a 1 cm^3 of a composite when filled with a fiber volume content of 60% contains as many as 3 million single filaments. The total area of the fiber surface is 3,400 cm^2. As a result, the matrix and its ability to adhere to a fiber are paramount to the effective transfer of the mechanical load in the composite (Erikson and Plueddemann 1974; Drza11983, 1986; Fishman 1991; Piggott 1991). The large surface area plays a direct role in the load transfer from the matrix to the reinforcing constituent. The way the interphase interacts with the matrix and with the fibers is quite important in determining damage initiation in composite materials and its ability to maintain sufficient impermeability to liquids and gases.

2.2 Strain-rate Effect and Microsturctural Failure

Micro structural study by Dutta et al (2000) of Gr/Ep composite fragments at CRREL, Hanover, NH and at the Air Force Wright Laboratory, Dayton, Ohio, has clearly shown that both temperature and the rate of loading significantly influence the interphase stress transfer mechanisms and final fracture that can influence the permeability as well as reliability in the performance of multiple launch. Reinforcing fibers and particles themselves may serve as stress raisers and lead to interfacial cracking (Eshelby 1957). Fiber-matrix debonding and cracks may significantly reduce the load transfer between matrix and the fibers and cause cracking in composites (Sottos, Li, and Agrawal 1994; Budiansky, Hutchinson, and Slutsky 1995). Interfacial damage (Keer, Dundurs, and Kiattikomol 1973; Hashin 1991; Pan, Green, and Hellman 1996) or material inhomogeneity of interphases also affects the elastic properties of composites (Jasiuk and Kouider 1993; Lagache et al. 1994; Low et al. 1995; Theocaris and Demakos 1995; Lutz and Zirnmennan 1996), the residual stresses (Jayaraman and Reifsnider 1993), and their macroscopic behavior (Tsai, Arocho, and Gause 1990; Kharik 1997; Kim and Mai 1991, 1998).

2.3 Residual Stress of Low-Temperature

Manufacturing of composites involves the use of a thermosetting polymeric material as the matrix phase. The polymeric matrix in the presence of a catalyst, heat, and pressure solidify through an irreversible exothermic chemical reaction (cure). Before curing, the polymer phase is a viscous fluid. It flows under pressure. As a result of curing, the polymer forms a covalently bonded three-dimensional molecular network with increasing viscosity and gel formation. The flow ceases at this stage but reactions continue to form a tightly cross-linked structure with characteristics of glassy solid (Rosen, 1993). The problem in composite cure is the problem of controlling the reaction exotherm and heat transfer so that uniform cure and minimum residual stresses are achieved (Bogetti et al. 1992). During the curing stage as the chemical reactions proceed residual stresses are developed with progressive changes in modulus and thermal expansion coefficients, and volume shrinkage of the resin. At the microstructural level

influence of low temperature on the induced stresses at the matrix/fiber interfaces, within the matrix, and in the interlaminar layers has been analyzed and experimentally investigated by many authors (Jones 1975, Lord and Dutta 1988, Dutta1988, Dutta and Lampo 1993). These results have shown that a difference between the curing temperature and the operating temperature may be as large as 200°C (392°F) in ususal cold environment, and the residual stresses may be sufficiently large to cause microcracking within the matrix and matrix/fiber interfaces. The computation of residual stresses using the Tsai and Hahn method (19) for unidirectional composites in longitudinal direction as:

$$\sigma_{mL} = (V_f E_f E_m)(\alpha_f - \alpha_m)(T - T_0)/(V_f E_f + V_m E_m) \qquad (1)$$

shows that at the cryogenic temperature of -180°C the matrix stresses could be as high as 12000 psi. Thus, the large residual stresses induced at lower temperatures become potentially damaging for polymer matrix composites with curing temperature environment. The damage may begin with the formation of microscopic cracks in the matrix or at the fiber/matrix interface. When these cracks develop to a certain density and size, they will tend to coalesce to form macroscopic matrix cracks (Wang, 1986). Transverse matrix cracking in composites affect stiffness, strength, dimensional stability, and fatigue resistance.

2.4 Fracture Toughness of Fiber/Matrix Interphase

An understanding of the failure process at the interphase at the cryogenic temperatures is essential to develop optimal performance capability at those temperatures. For this, one must closely examine the polymer matrix and its interaction with the interfacial surfaces (Wool 1995; Hrivnak 1996),). Many studies, as reviewed by Cantwell and Morton (1991), have concluded that composites are particularly susceptible to damage by delamination, which is particularly dangerous because it is often not visible from surface. The composites property measured in the fracture mechanics study of the resistance to delamination is the critical energy release rate, or fracture toughness, which is a measure of the energy consumed during the creation of unit area of fracture surface during delamination. Three modes of crack loading can occur, namely mode I (tensile opening), modeII (in-plane shear) and mode III (out-of-plane shear). In practice, modes I and II and combinations of mode I and II are the most important.

Test methods for measuring the interlaminar fracture toughness (K_C) at slow rate in mode I, II and mixed I/II are well established and several standards exist for mode I (ASTM D5528, ASTM E399, ISO CD 15024 version 97-02-24, and JIS K 7086 of 1993). Various test methods are currently being pursued for the other modes. However, currently no appropriate high rate-loading test, especially under cryogenic conditions exists, and all previous attempts to extend the slow speed test methods to high rates have met with significant obstacles (Blackman and Williams 1998). The first obstacle is in experimental test equipment to be capable of rapidly accelerating the test specimen

and then accurately recording the forces applied and the deformation occurred. Second, the dynamic effects are invariably induced at the high rate tests and it is critical that these effects are carefully considered, and accurately accounted for, if accurate and valid K_C values are to be measured. Indeed, this probably accounts for the conflicting nature of some of the test results reported in the literature. For example, Smiley and Pipes (1987) pointed to very large reductions in the values of K_{IC} of K_{IIC} for brittle epoxy as well as for thermoplastic polyether etherketone (PEEK) composites, as the test rate was increased from a few mm/min to about 1m/s. On the other hand, Beguelin et al (1991) reported mode I results of a PEEK matrix carbon composites only a small reduction in the value of K_{IC} as the test rate was similarly increased. In a third study by Aliyu and Daniel (1985) on similar materials, increasing followed by decreasing values of K_{IC} was reported as the test rate was increased. The differences in experimental results reported were further highlighted in a recent review by Cantwell and Blyton (1998). Their review indicated that the rate sensitivity of the composites was dominated by the toughness of the matrix, with brittle matrix composites exhibiting much less of a rate effect than tough matrix composites.

3. EXPERIMENTAL STUDY

We have undertaken the experimental study to determine how the composites behavior change as we approach the cryogenic temperature range by performing five series of tests: (1) Shear response at cryogenic temperatures, (2) Microfracture growth monitoring by acoustic emission as the temperatures are reduced, (3) Modulus degradation evaluation by ultrasonic wave transmission (pulse-echo) method, (4) Shear property degradation by short beam shear property evaluation, and by (5) fracture properties over a wide strain rate and temperatures.

3.1 Shear Response at Cryogenic Temperatures

These tests were performed to study the effects of temperature on the interlaminar shear resistance. The range of temperature was varied from -100^0C to 80^0C. The results showed a drastic reduction of interlaminar shear strength with the temperature rise from 50^0C to 80^0C.However the increase in the shear strength with decreasing temperature is more gradual. The test specimens were prepared from a pultruded glass fiber reinforced composite square bar of 0.5 in. × 0.5 in. section. From this stock the specimens were machined with the fibers oriented in longitudinal direction. The rectangular specimens had a dimension of 1.5 in × 0.5 in × 0.25 in. Figure 1 shows a typical specimen. These specimens were then tested for interlaminar shear strength using the ASTM D2344-84 (The ASTM standard D2344-84 specifies the span to thickness ratio of 5. In our case the ratio is 3.26.

3.1.1 Testing

The tests were performed in an environment chamber which could be cooled with liquid nitrogen, or heated by a heating coil. The cooling system involves a supply of liquid nitrogen from the commercially available liquid nitrogen tank through a control valve which releases the evaporated liquid nitrogen into the environment chamber. A feedback loop of temperature sensed by a thermocouple controls the release of liquid nitrogen so that the temperature inside the chamber is maintained steady within +/- 1 ^{0}C.

The chamber could also be heated to a higher temperature by the heating coil mounted inside the test chamber. Figure 2 shows the test chamber with the heating coil. Again a feed back loop control using the thermocouple controls the temperature of the chamber.

For testing at temperatures other than the room temperature the specimens were soaked at that temperature for a minimum of 45 minutes. The short beam shear test was performed in a MTS machine using the Wyoming test fixture for three point bending.

3.1.2 Test Results

Table-1 shows the results of the test. Figure 3 shows the variation of the shear strength with temperature. Figure 4 shows the force displacement curves at different temperatures. Figure 5 shows the displacement at peak load at different temperatures.

3.1.3 Discussion

From Figure 3 we see that there is a drastic decrease of shear strength with increasing temperature from 23^{0}C to 80^{0}C. Possibly the higher temperature softened the matrix of the composite. From 23^{0}C to   -100^{0}C we observe that the shear strength increases linearly. However this increase is more gradual. The increase in strength with temperature reduction can be modeled by the following equation:

$$S_H = -15.7494 \, T + 8935.36 \qquad (2)$$

Where S_H = Shear Strength (psi), T = Temperature (°C)

Figure 4 gives the force-displacement curves. Figure 5 shows that the displacements at peak load decreases with decreasing temperature. Also the peaks are not sharp at higher temperatures (Figure 4). The sharp peaks at lower temperature denote brittleness of the material. We conclude that (1) Shear Strength decreases drastically with increasing temperature. (2) At low temperatures shear strength increases almost linearly. (3) The material becomes more brittle at lower temperatures as seen by reduced deflection and sharp peaks.

Table 1. Temperature effect on Shear Strength in Quasi Isotropic test

Temp. (°C)	No. of Samples	Shear Strength S_H (psi)	Displ. at peak load (in)	Standard Deviation

- 100	6	10510.8	0.020	349.7
- 5	6	9014.6	0.021	365.9
23	6	8309.8	0.022	288.0
50	6	4926.2	0.031	195.0
80	6	2721.8	0.051	96.2

Figure 1 The view of interlaminar shear test specimen

Figure 2 The test chamber with the heating coil
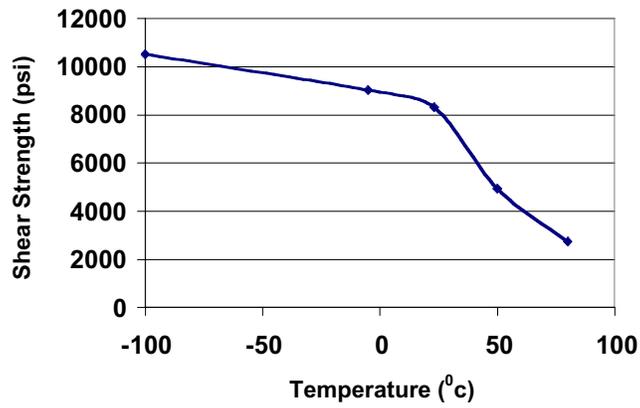
Figure 3. Variation of the shear strength with temperature
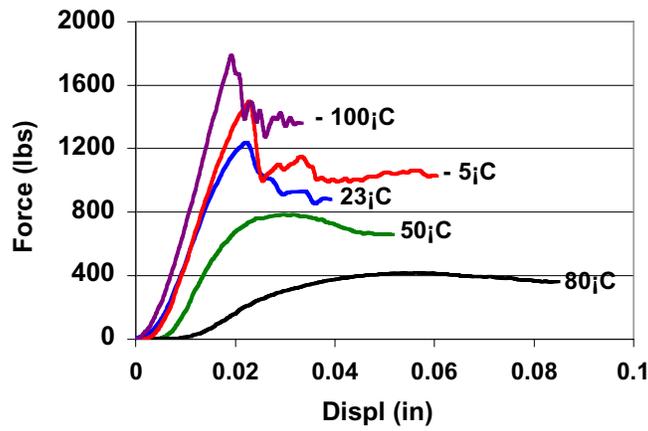
Figure 4 Force vs displacement at different temperatures
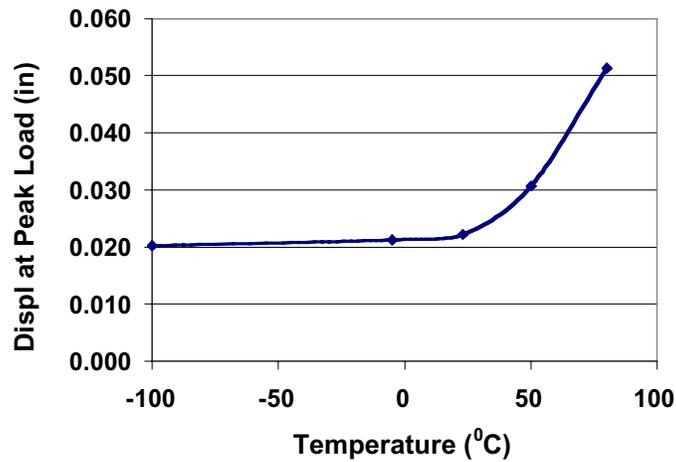
Figure 5 Variation of displacement at peak load with temperature

8

4. CRYOGENIC FRACTURE TOUGHNESS

The plain strain fracture toughness is the stress concentration at the crack tip under conditions of plane strain, and is regarded as the basic material property. The fracture toughness was determined by applying bending load to the notched specimens as shown in Figure 6.

4.1 Specimen Dimensions

The material of test specimen is a commercial pultruded composite product, which uses E-glass fiber and isophthalic polyester resin. The details of the test material are given in Table 2 and Figure 7.
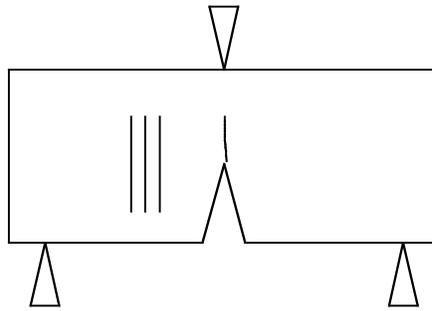
Figure 6 Test configurations for the Fracture Toughness Test

Table 2 The specification of test material

E-glass FRP composite
Used Process: Pultrusion method
Reinforcing Fiber: E-glass
Matrix: Polyester
Density: 0.071 lb/in^3 (0.971 g/cm^3)
Volume Fraction of Fiber: 0.593
Notch angle: 90 degree
Dimensions: -
Length: 1.511in (38.38mm)
Width: 0.494in (12.55mm)
Thickness: 0.521in (13.23mm)
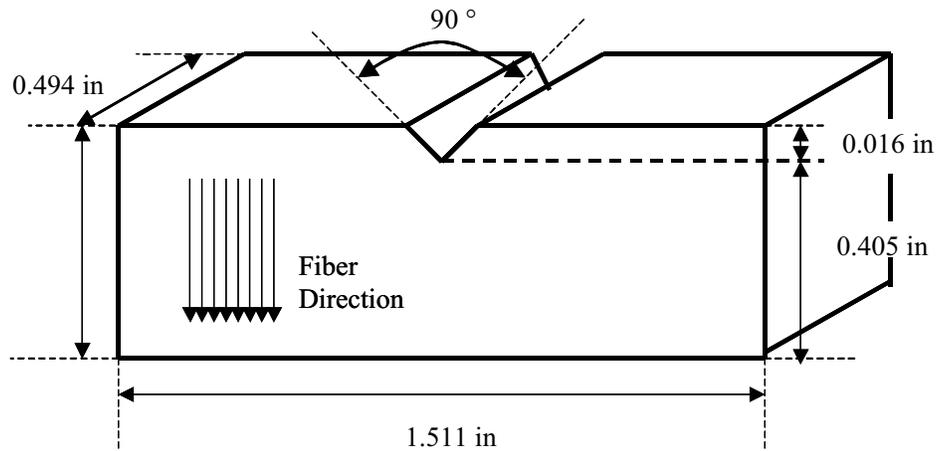
Figure 7 Schematic of the composite test specimen

4.2 TESTING

The speciemens were tested both quasi statically and dynamically using the ASTM D70 three point-bending test.

4.2.1 Quasi-static Tests

Quasi-static tests were performed on the glass fiber specimen of 90-degree fiber orientation at room temperature (23 C) and at low temperature (-30C) with a servo controlled hydraulic testing machine driving the loading platen at a speed of 0.01 inch/min. An environmental chamber was used for all low temperature tests. The chamber was cooled with chilled nitrogen gas slowly vented through a regulating valve controlled by a temperature sensor near the test specimen. Tests were performed only when a stable temperature was established for about 15 minutes within the chamber. Load and displacement were recorded using the load cell and the LVDT transducer attached to the testing systems and the data were automatically transferred to the same digital data acquisition system.

4.2.2 Dynamic Test

4.2.2.1 Experimental Approach

We performed a study of the interlaminar Mode I fracture toughness, K_{IC}, of unidirectional composites at room and cryogenic temperatures using a modification of Split Hopkinson Compression Bar Apparatus (SHBA). By using SHBA we had overcome the difficulties encountered by the researchers in measuring loads and deformation while using the traditional servo hydraulic machines at rate above 1m/s. SHBA would allow a rate up to 100m/s. The past researchers did not take into account the problems of low temperatures associated with high rate loading.

Our approach to measure the cryogenic high-strain-rate fracture toughness for composites is new and unique. The details of the proposed system, a preliminary model of which has already been developed, is shown in Figure 8(a) and 8(b). The typical stress waves used for computation of the force-displacement curves are shown in Figure 8(c). As shown in this Figure, we modified the SHBA interface to represent a three-point loading system of a single notch prismatic composite sample, which is mounted in between the two interfaces of the SHBA. The intact and the fracture samples are shown in Figure 9. Figure 10 shows the sample in the SHBA set up, and Figure 11, the cryogenic cooling with liquid nitrogen. The entire fracturing process would be performed in a cryogenic chamber built around the SHBA interfacial impact zone. We plan to measure the crack opening force and the corresponding displacements exactly the same way as we do in a standard Hopkinson Bar by integrating the incident, reflected and transmitted strain waves in each bar (Dutta 1987). The system will allow K_{IC}. to be measured with samples in which fiber orientation is parallel to the notch axis.
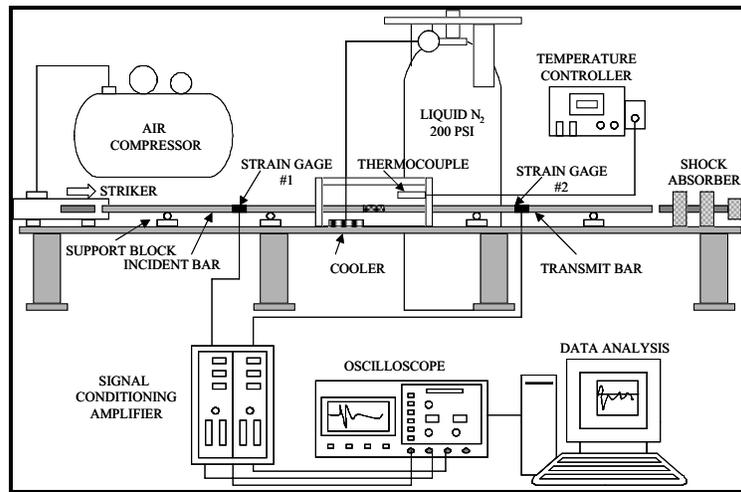
(a) Split Hopkinson pressure bar system schematic

(b) CRREL Split Hopkinson Bar apparatus

11
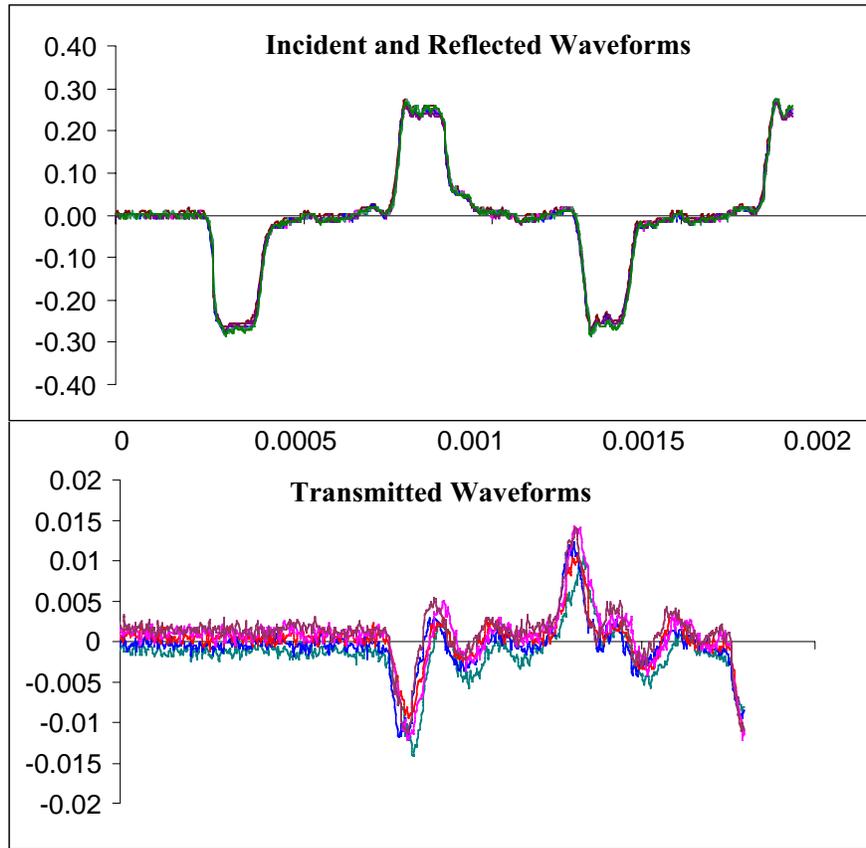
(c) Incident and Reflected Waveforms for five tests

Figure 8. The Cryogenic SHBA experiment

4.2.2.2 Analytical approach

For a specimen in three point loading (Figure 3), K_{IC} is calculated using the expression of Brown and Strawley (1966),

$$K_{IC} = \frac{6M}{Bd}\sqrt{a}F(a/d)\cdots\cdots$$

$$M = Pl/2$$

where $F(a/d)$ is the finite width correction factor given by $F(a/d) = 1.99-2.47(a/d)+12.97(a/d)^2-23.17\ (a/d)^3+24.80(a/d)^4$

where a = crack length, d = specimen depth, M = ultimate bending moment, P = applied load, l = shear span, and B = specimen width.

4.2.3 RESULTS AND DISCUSSION

Quasi static test at room temperature gave the K_{IC} value of 6.9 ksi√in. The batches for dynamic test of the notched samples (Figure 9(a)) were tested at different temperatures. A representative specimens which failed under the dynamic tests is as shown in Figure 9(b).
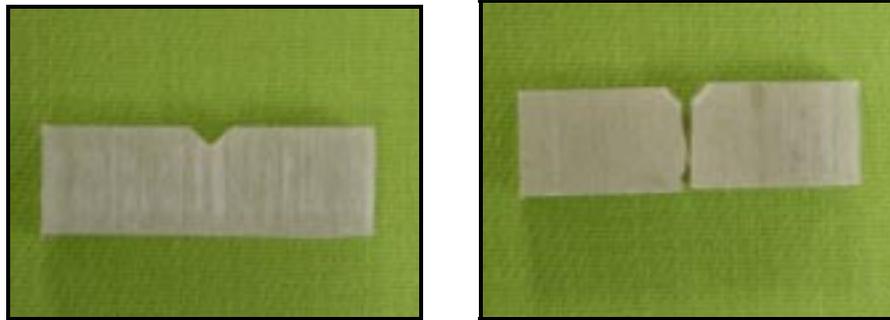
(a) Sample before test   (b) Sample after test

Figure 9 GFRP samples before and after dynamic test
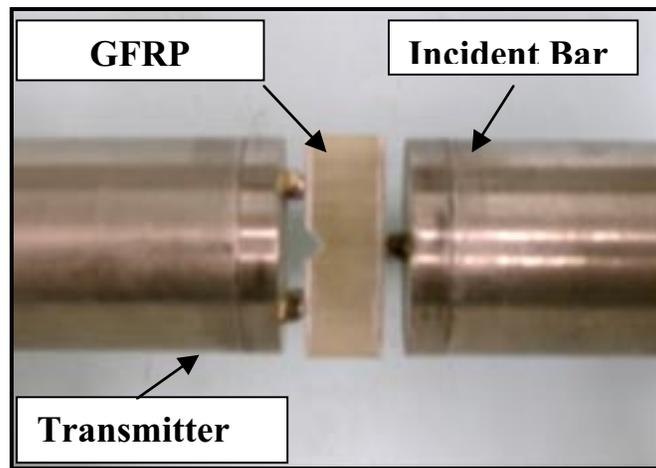
Figure 10 Loading position of the specimen

Figure 11. The chamber used to keep the test specimen cold

It is clear that there are multiple cracks along the fracture path in the test specimens. No significant differences in the crack patterns were observed between high temperature and low temperature fracturing. The force-displacement characteristics and then the energy absorbed to develop the crack were determined. The absorbed energy versus time plot at different temperatures are shown in figure 12.
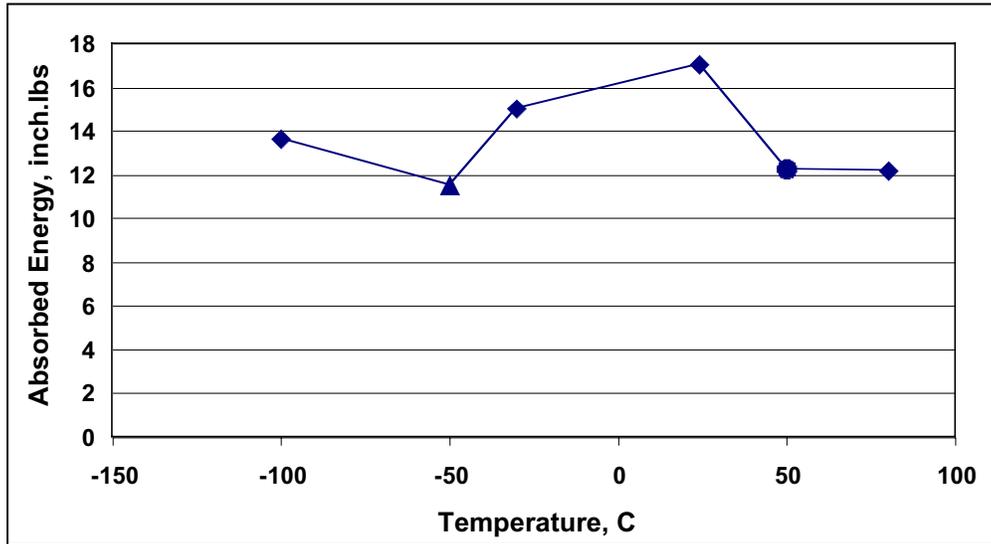
Figure 12. Average energy absorbed at different temperatures

From Figure 12 we observe that the energy absorbed within the system is higher at –30 C and room temperature as compared to –50 C and 80 C.

The force-displacement curve showed a dramatic increase in stiffness and brittleness of both specimens in dynamic fracturing**.** The displacement at the peak force was assumed as the fracture initiation point. Because of the visco-elastic nature of the composite matrix, we do not always find any sharp failure point. At this point, there is considerable amount of scatter for the peak force. This is expected in Extren, which is a pultruded composite in which fiber volume percentage is low and many resin-rich areas occur. The peak force was used to calculate the fracture toughness, K_{IC}. The calculated values of K_{IC} are summarized in Table 3 and plotted in Figure 13.

Table 3: Summary of result of fracture toughness

Temperature (°C)	Avg. Maximum Energy (inch. lbs)	Avg. Maximum Displacement (in.)	Avg. Maximum Force (lbs)	Avg. Fracture Toughness (Ksi.√in)
80	20.29	0.01259	1321.0	6.114
50	12.38	0.01217	1398.7	6.000
24	19.82	0.00630	1359.7	6.900
-30	14.03	0.01349	1126.6	5.307
-50	11.82	0.00821	893.4	5.146
-100	13.61	0.00515	1476.4	4.381
-150		0.00561	1262.5	3.746

y = 6.1431e0.0029T
R2 = 0.9599
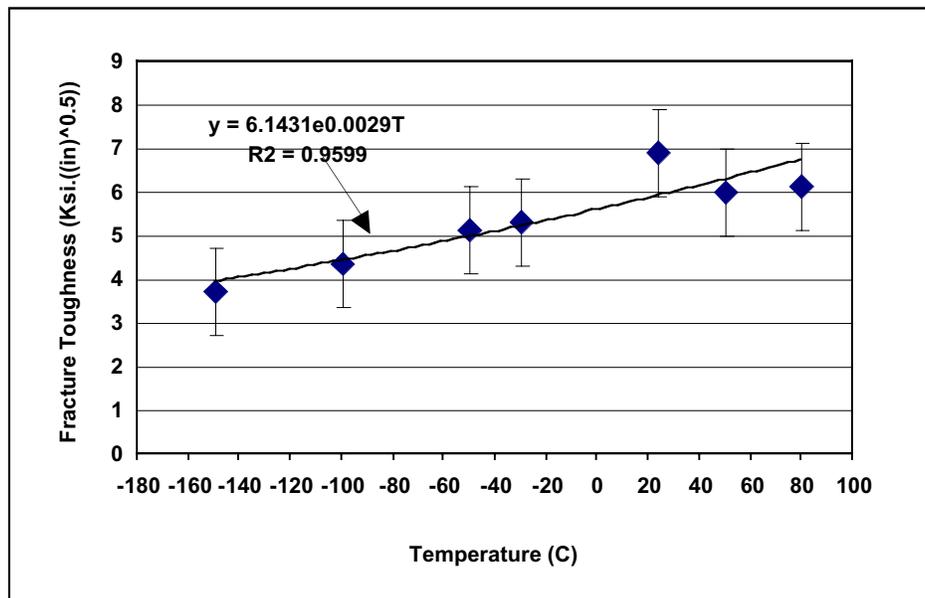
Figure 13 Fracture Toughness at different Temperatures

The K_{IC} values were plotted against the test temperatures. It is seen from the graph that fracture toughness varies with temperature. K_{IC} increase with increase in temperatures. As

stated before, many factors contribute into the value of K_{IC} for a given material. The strain rate data is summarized in the Table 4.

Table 4 Strain rate at different temperatures.

Temperature (˚C)	Avg. Maximum Force (lbs)	Strain	Strain Rate (Strain/sec)
80	1320.9	3591.75	49.885
50	1398.6	3803.03	52.819
24	1359.6	3696.94	51.346
-30	1126.6	3063.24	42.545
-50	893.4	2429.15	33.738
-100	1476.3	4014.31	55.754
-150	**1262.5**	**3432.73**	**47.676**

It is concluded that the low temperature reduces the fracture toughness of the compsites. However fracture toughness increase with increase in temperature with the average strain rate of 40 ~ 50strain/sec. The strain rate was calculated by assuming that the maximum force reached the value at approximately 72 microseconds. The maximum value of force was considered applied to load a bending. Low temperature influence the energy absorption characteristics of the GFRP, i.e. it absorbs less energy at low temperatures as compared to high temperatures. After the fracture of the specimen, multiple cracks were observed along the fracture path but it was found that there is no significant difference in crack pattern between low and high temperatures.

5. Acoustic Emission Study

We hypothesized that the growth of microcracks in composite are likely to happen when the temperature is lowered to the cryogenic range.

5.1 Procedure for Acoustic Emission test

The procedure for the acoustic emission test is described below.

A 50-ply carbon test sample of size 4"length, 0.75"width and 0.25" thickness is taken and a transducer is placed on the sample. Vacuum grease is used as a fluid between the sample and the transducer to ensure the proper transformation of signals from sample to transducer. The transducer is then clamped tightly (Figure 14) with sample so that it does not move during the test. A thermocouple is clamped with specimen to note the

temperature of sample. The thermocouple is connected to a datalogger, which reads the temperature of specimen for every 2 or 4 sec and sends the data to a computer. The software used for this is called CAMPBELL SCIENTIFIC software.
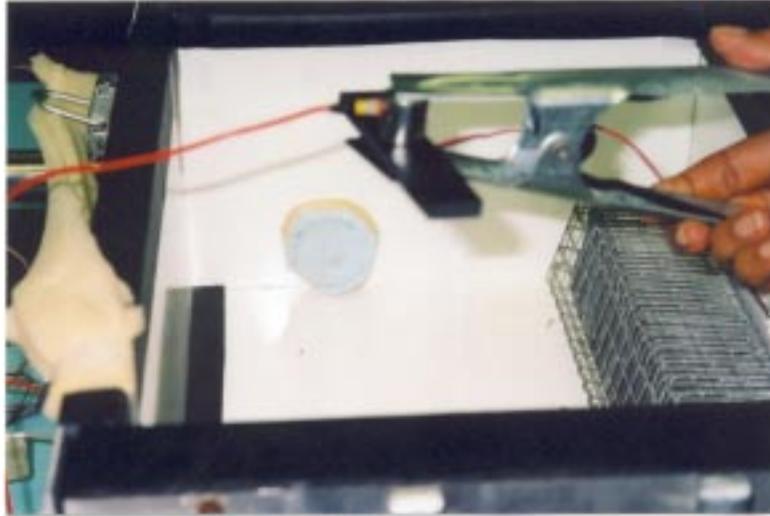
Figure 14 Clamping of the transducer for acoustic emission test

The specimen is kept in a test chamber which was cooled by liquid nitrogen The transducer collects the data of the time and accumulated events whenever an event occurs on the specimen.(i.e. when ever the specimen has micro cracks).

The software used to record the events data is MISTRAS software of PHYSICAL ACOUSTIC EMISSIONS CORP. The sample is subjected from room temperature to low temperatures (23,-5,-50,-100, and -150C) and kept at each of these temperatures for approximately 10 minutes, then the temperature was raised from –150C to room temperature. The data of time,events and temperature is recorded throughout.

Graphs were plotted between the time vs temperature and time vs accumulated events (Figure 15). We observe that the rate of events increases from room to low temperatures but from -150C to room temperature, the rate of increase of events is very low. This indicates that the cracks produced were high during the first half of the test and less during the second half of the test.
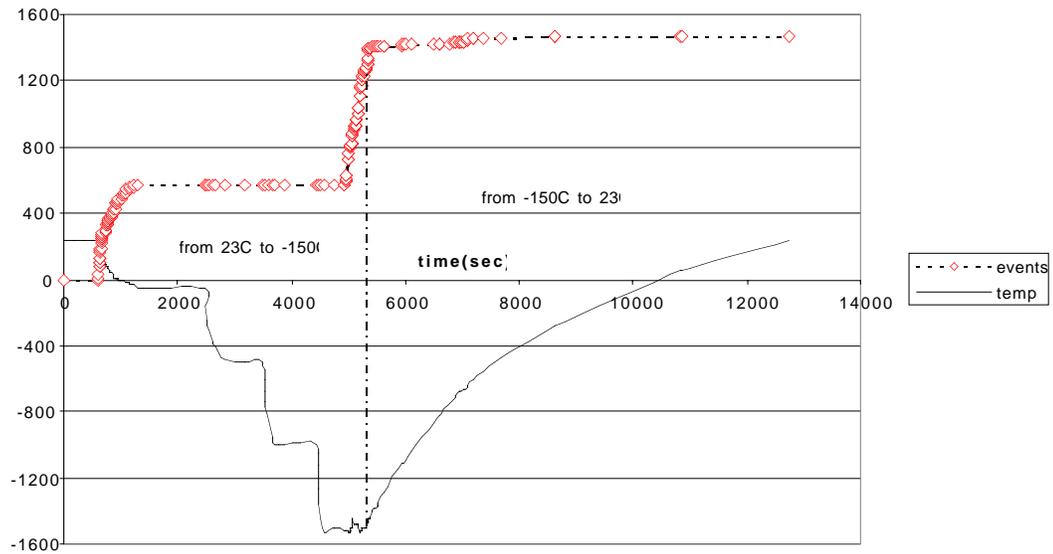
Figure 15 Increase in acoustic events with temperature

5.2 Results

Maximum no. of events counted for each sample is given in Table 5.

Table 5 Maximum no. of acoustic emission events

Samples	Temp (°C)	Max no. of events on lowering of temperature	Max no. of events on warming to room temp
1	-161	1492	---
2	-154	1930	33
3	-150	1280	186
4	-150	3789	82
5	-150	3495	249

6. Ultrasonic test evaluation at cryogenic temperature

6.1 Liquid nitrogen immersion test

In the first series of tests composites samples were immersed in liquid nitrogen (Temperature, – 196 C) for different durations. The samples, immediately (within 5 to 10 seconds) after removal from the liq Nitrogen bath were tested for determining the ultrasonic velocities (Figure 16(a)). Figure 16(b) shows the velocity measurement by the ultrasonic technique. The same samples were again tested for velocities when they achieved the room temperature after a day. Table 6 shows the immersion times vs velocity and Young's modulus. The results are also shown graphically in Figure 17. Figure 18 and 19 shows the Young's modulus of each speciemen.

Table 6 Immersion and rapid test data

Temperature (°C)	Immersed Time (min)	Velocity at cryogenic temp immediately after removing from Liq Nitrogen (m/s)	Velocity at room temperature long after removing from Liq Nitrogen (m/s
	60	2559	2248
	45	2559	2255
	30	2559	2294
Cryogenic (-190)	15	2511	2306
	5	2464	2368
Room (24C)	None	2376	2376

(a) Ultrasonic testing machine
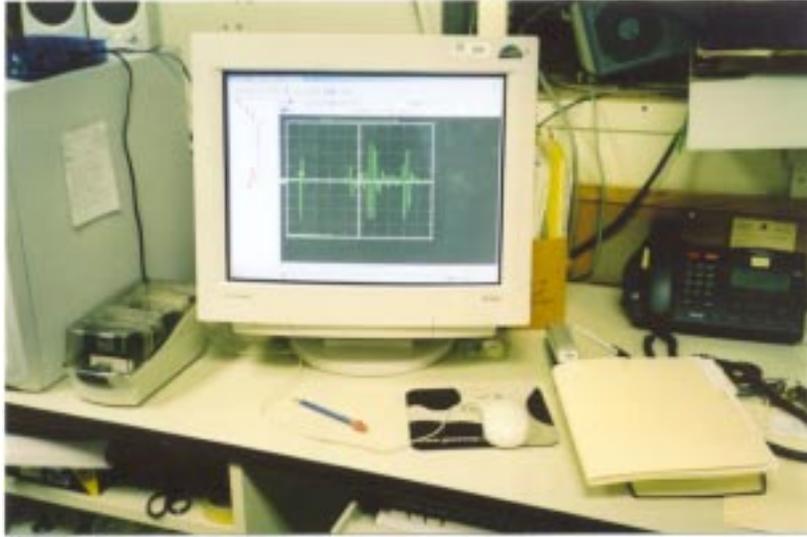
(b) pulse-eco signals in the ultrasonic testing

Figure 16 Ultrasonic testing technique
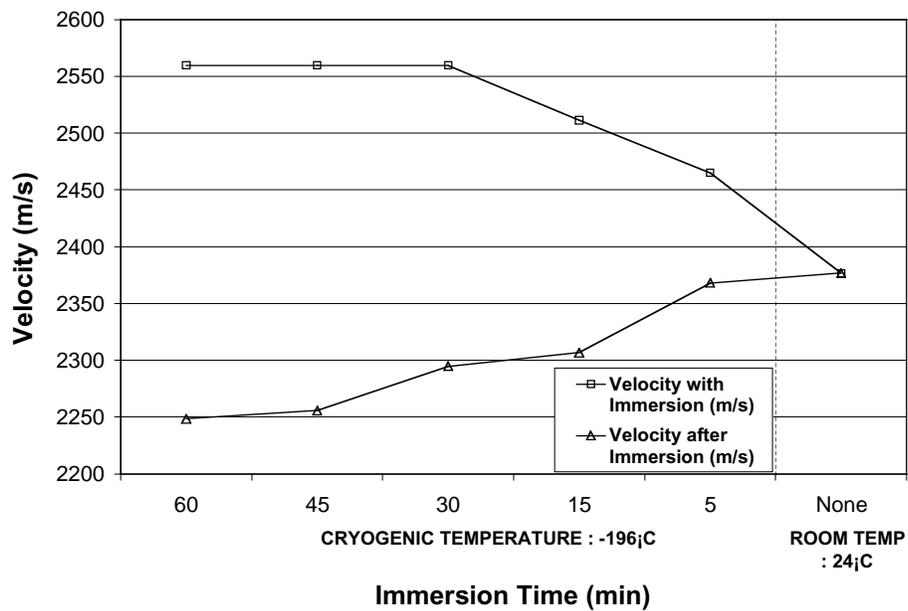
Figure 17 Change of velocities with different immersion times in Liq Nitrogen. The point at right shows the room temperature velocity data.
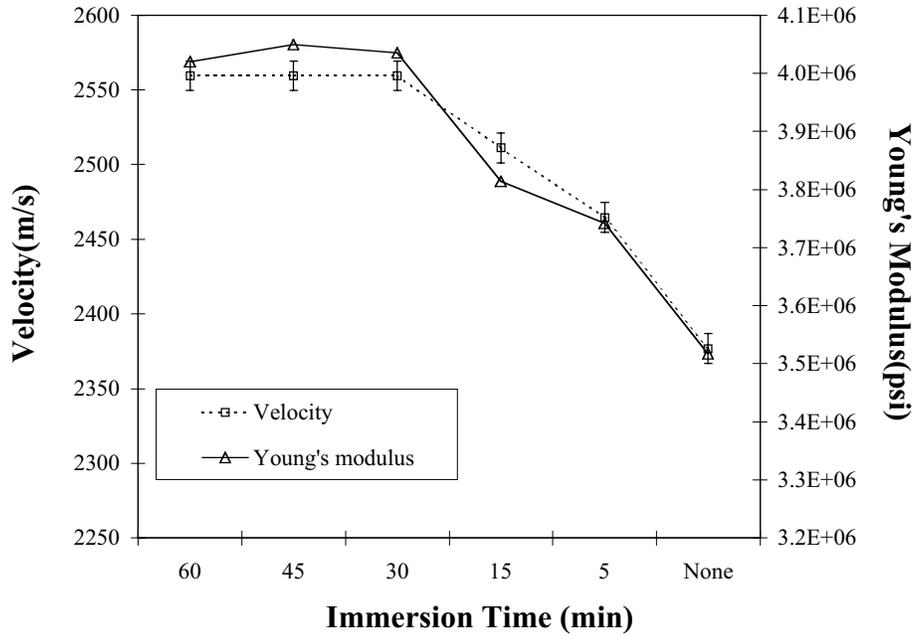
Figure 18 The Young's modulus of CFRP specimens just after the immersion test
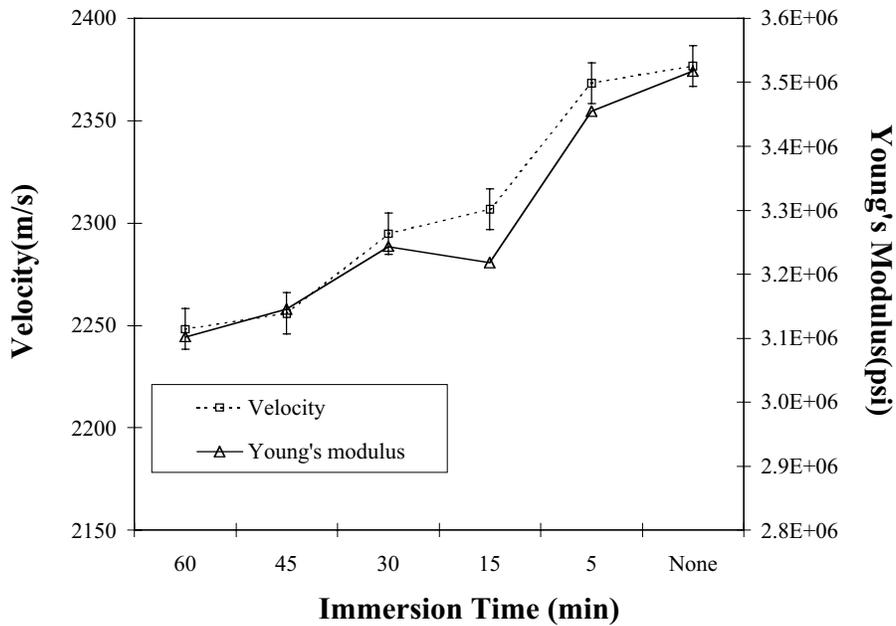
Figure 19 The Young's modulus of CFRP specimens that kept it at room temperature for 2 days after the immersion test

6.2 Room and Liquid Nitrogen Comparison Test

In the second series of tests one composite sample was first tested for the velocities at room temperature. And then the sample was immersed in liquid nitrogen, and kept immersed for one hour. Then the sample was taken out and tested for acoustic emission till the specimen achieved room temperature. The specimen was again tested for velocity. Figure 20 shows the acoustic emission results. Figure 21 shows the results of the velocity and Young's modulus of CFRP sample after immersion test.
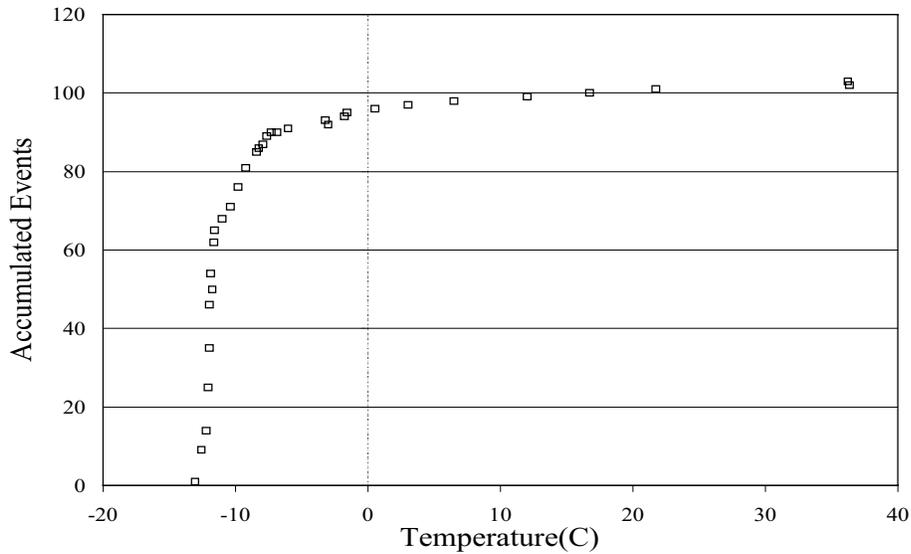
Figure 20 The acoustic emission results
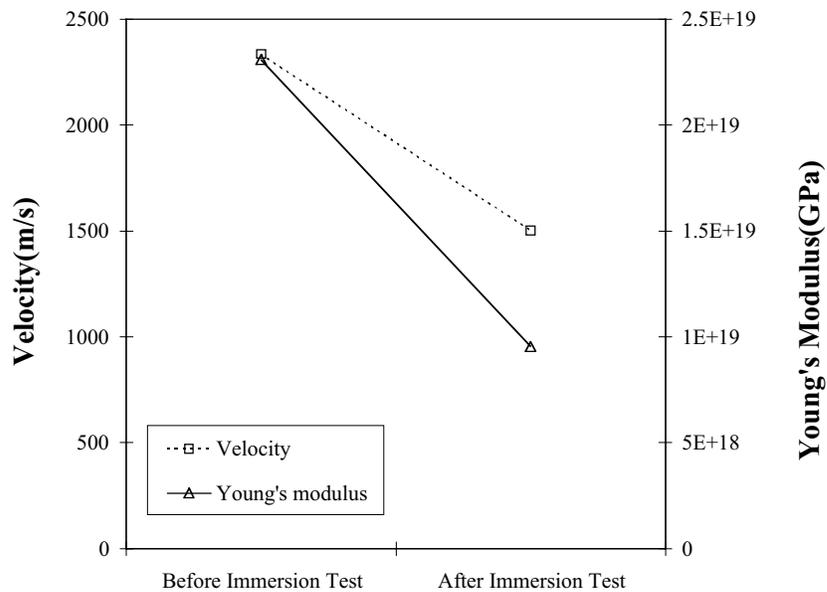
Figure 21 The results of velocity and Young's modulus after immersion test

6.3 Ultrasonic evaluation of cryogenically exposed samples

In this series of tests ultrasonic velocities were determined for all samples, which were subjected to the acoustic emission tests. The results are given in Table 7. Note that there is asmall change in the velocities after exposure to the liquid nitrogen, which can account for the microcrack generated emissions from the composites when cooled.

Table 7 Velocities after the exposure to cryogenic temperatures

Sample #	Velocity (m/sec)
1	2713
2	2721
3	2721
4	2713
5	2713
Average	2716

Note that before immersion, the room temp velocity was 2737 m/sec (average of 3 samples). The average velocity after the exposure was 2716, a reduction of 21 m/sec for the damage growth.

7. CONCLUSIONS

Cryogenic exposure of graphite epoxy and other composites show that residual stresses at the fiber matrix boundary and at the interlaminar zone increase significantly. The increase may be sufficient to develop microcracks, which can be monitored by acoustic emission. Degradation of interlaminar shear strength is not sufficient, rather the low temperature increased the strengths. However, the fracture toughness decreased with lowering of temperatures. The degradation was also noticed by decrease in ultrasonic velocities.

The results presented here are mostly preliminary. As the testing are going on, more data are expected and characterization at the cryogenic temperatures will be more certain.

7. ACKNOWLEDGMENT

8. REFERENCES

1. Brown, W. F. (1970) "Review of Developments in Plane Strain Fracture Toughness testing," ASTM STP 463.

2. Dorn, John E. (1961) "Mechanical Behavior of Materials at Elevated Temperatures," McGraw-Hill Book Company, Inc.

3. Dutta, Piyush K. (1988) "Hopkinson Pressure Bar Data Acquisition and Analysis Methods," CRREL Technical Report

4. Dutta, Piyush K. and David Hui (1996) "Low-Temperature and Freeze-Thaw Durability of Thick Composites," COMPOSITES: PART B, Vol.27B, No.3/4, pp.371-379

5. Dutta, Piyush K., Dennis Farrell and John Kalafut (1988) "Hopkinson Pressure Apparatus- A Tool for Rapid Assessment of Material Properties at High-Strain Rates," Proceedings of TEST TECHNOLOGY SYMPOSIUM I, Volume II, J-20

6. Dutta, Piyush K. David Hui and Magna R. Altamirano (1991) "Energy Absorption of Graphite/Epoxy Plates Using Hopkinson Bar Impact," CRREL Report 91-20

7. Dutta, P. K. D. Hui and Akshay Patil (2001) "High-Strain-Fracture Energy of Unidirectional Composites," ICCE-8

8. Dutta, P.K., Mamidi Kumar, David Hui. (1994) "Dynamic Tensile Strength of Glass Fiber Reinforced Pultruded Composites," Page 357-363, ASME PD Vol. 62, Materials and Design Technology.

9. Dutta, P. K. (1994) "Low-Temperature Compressive Strength of Glass-Fiber Reinforced Polymer Composites," Journal of offshore Mechanics and Arctic Engineering, Vol. 116 , pp.167-172.

10. Dutta P. K., David Hui and Rathi Bhattacharya (1995) "On the Effects of Moisture and Low Temperature on Polymeric Composites," SES'95, 32nd Annual Technical Meeting, New Orleans, LA.

11. Dutta, Piyush K. and David Hui, (1995) "Low-Temperature High-Strain-Rate Behavior of GR/EP Laminate Under Transverse Impact," Advanced Structural Fiber Composites, pp. 455-468.

12. Dutta, Piyush K., (1993) "Compressive Failure of Polycrystalline Ice Under Impact," Proceeding of 3rd International Offshore and Polar Engineering Conference, Singapore, pp. 573-580.

13. Flaggs, D. L., (1985) "Prediction of Tensile Matrix Failure in Composite Laminates," Journal of Composites Materials, Vol. 19, pp.29-50.

14. Hann, H. Thomas, (1976) "Residual Stresses in Polymer Matrix Composites Laminates," J. Composite Materials, Vol. 10, pp. 226-278.

15. Hertzberg, Richard W., (1989) "Deformation and Fracture Mechanics of Engineering Materials," 3rd Edition, John Wiley & Sons.

16. Hui, David and Piyush Dutta, (1992) "Stress Wave Propagation through the Thickness of Graphite/Epoxy Laminated Plate Using PVDF Sensors," 6th Japan-US conference on Composites Materials, Orlando, FL, pp 845-854.

17. Hui, D., A. Patil. and P. Dutta, (2002) "Effects of Temperature on Fracture Toughness of Glass Fiber Reinforced Polymer (GFRP)," ICCE/9, July 2002

18. Jones, Robert M., (1975) "Mechanical of Composites Materials," Hemisphere Publishing Corporation.

19. Liebowitz., (1969) "FRACTURE: An Advanced Treatise," Volume IV Engineering Fracture Design 1969, Academic Press

20. Lord, Harold W., (1988) "On the Design of Polymeric Composite Structures for Cold Regions Applications, " Journal of Reinforced Plastics and Composites, Vol. 7, pp. 435-458.

21. McClintock, Frank A. and Ali S. Argon, ( ) "Mechanical Behavior of Materials," Addison-Wesley Publishing Company, Inc., Addison-Wesley (Canada) Ltd.

22. Nairn, J. A., (1997) "Fracture Mechanics of Composites with Residual Thermal Stresses," Journal of Applied Mechanics, In Press/1-11

23. Nwosu, Sylvanus N., Piyush K. Dutta, and David Hui, (1994) "Stress Wave Propagation in Rocks and Unsolidated Soil Samples by Vertical Dynamics Hopkinson Bar," ICCE/1, pp. 373-374.

24. Nwosu, Sylvanus N., Piyush K. Dutta, and David Hui, (1994) "Characterization of Composites Materials by Vertical Dynamics Hopkinson Bar," American Society of Mechanical Engineers, pp. 141-151.

25. Nwosu, S. N., S. K. Sivapuram, P. K. Dutta and D. Hui, (1995) "Hopkinson Bar Performance of Laminated Composites" ICCE/2, New Orleans, LA, pp.559-560.

26. Rolfe, Stanley T. and John M. Borsom, (1977) "Fracture and Control Fatigue in Structures: Applications of Fracture Mechanics," Prentice Hall, Inc., Englewood Cliffs, New Jersey

27. Springer, George S. (1988) "Environmental Effects on Composite Materials," Vol. 3, Technomic Publishing Co. Inc.

28. Standard Test Method for Plane-Strain Fracture Toughness of Metallic Materials, Designation: E399- 90

29. Sun-Pui Ng, Piyush K. Dutta and David Hui, (1999) "Energy Balance in Hopkinson Bar Under Oblique Impact," ICCE/6, Orlando, Florida, pp.675-676.

30. Soutis, C. and D. Turkmen "High Temperature on the Compressive Strength of Glass Fiber Reinforced Composites", ICCM-9 COMPOSITES: Properties and Applications Vol. VI, pp. 581-587.

31. Smiley, A. J. and R. B. Pipes (1986) "Rate Sensitivity of Inter-Laminar Fracture Toughness in Composites Materials," Proceeding of American Society of Composites, 1st Technical Conference, pp. 434-449.

32. Taya, Minoru and Tsu-Wei Chou, "Prediction of the Stress-Strain Curve of a Short-Fiber Reinforced Thermoplastic," Journal of Materials Science 17, pp. 2801-2808.

33. Takao, Y., T. W. Chou, M. Taya, (1982) "Effective Longitudinal Young's Modulus of Misoriented Short Fiber Composites," Transactions of the ASME, Vol.49, pp.536-540.

34. Vaidya U.K., M. Kulkarni, M.V. Hosur, Arnold Mayer and Piyush Dutta, (2001) "High Strain Rate Impact Response of S2-Glass/Epoxy Composites with Polycarbonate Facing," Polymers and Polymers Composites, Vol. 9 No. 2, pp. 67-79.

35. VanDerSluys, W. A., B.A. Young, D. Doyle, and P. Neubrand, (2000) "Dynamic Fracture Toughness Results of High Strength Pressure Vessel Weldments in the Brittle-to-Ductile Transition Region," ASME Pressure vessel and Piping Conference, Seattle, Washington, MTI 00-02 pp.1-6.

36. Warren, P.D., (1995) "Determining the Fracture Toughness of Brittle Materials by Hertzian Indentation," J. Euro. Ceram. Soc, 15, pp. 385-394.

37. Aliyu A.A., and Daniel, I.M.,Effects of Strain Rate on Delamination Fracture Toughness of Graphite Epoxy, Delamination and Debonding of of Materials, ASTM STP 876, Philadelphia, 336-348, (1985).

38. Ashby, M.F.FRS, Easterling, K.E., Harryson, R., and Maiti, S.K., The Fracture and Toughness of Woods, Proc. Royal Soc. London, A398, pp 261-280 (1985).

39. Beguelin, Ph, Barbezat, M., Kausch, H.H., Mechanical characterization of Polymer Composites with Servo hydraulic high speed tensile tester, J. Physics, III France !, 1867-1880, (1991)

40. Blackman B.R.K., Dear J.P., Kinloch, A.J., McGillivary, H., Wang, Y., Williams J.G., Yala, P., The Failure of Fiber Composites and Adhesively Bonded Fiber Composites under High Rates of Test, J. Mater. Science, Vol 31, 4467-4477, (1996).

41. Brown, W.F., and Strwley, J.E., in Plane Strain Crack Toughness Testing of High Strength Metallic Materials, ASTM STP410, ASTM, Philadelphia p.11, 1966.

42. Cantwell, W.J. and Morton J. The Impact Resistance of Composite Materials – A Review, "Composites", Vol 22, No. 5 (1991)

43. Cantwell, W.J. and Blyton P., A Study of Skin –Core Adhesion in Glass Fiber Reinforced Sandwich Materials, Applied Composite Materials, Vol 3, pp 407-420, (1998).

44. Drzal, L. T. "Composite Interphase Characterization. SAMPE Journal, pp. 7-13, September/October,1983

45. Dutta, P.K., Hui, D., Kadiyala, S.V., A Microstructural Study of Gr/Ep Composite Material Subjected to Impact, Computers and Structures, Elsvier Science Ltd pergamon, Vol 76, pp 173-181, 2000.

46. Dutta, P.K., Farrell, D, Kalafut J., (1987) The CRREL Hopkinson Bar Apparatus, CRREL Special Report.

47. Smiley, A.J., and Pipes, R.B., Rate Effects on Mode I Interlaminar Fracture Toughness in Composite Materials, J. Composite Materials, Vol 21 (7), pp 670-687, (1987)

48. Sih, G.C., Paris, P.C. & Irwin,G.R., Int. National Journal of Fracture Mechanics, , Vol 1, p 189, 1965.,

49. Wool, R. P. polymer Interphases. Munich: Hanser, 1995.